Observational Investigations of Entrainment Within the Weak Echo Region

KENNETH L. GRANDIA[1] AND JOHN D. MARWITZ

Department of Atmospheric Science, University of Wyoming, Laramie, Wyo. 82071

(Manuscript received 18 August 1974; in revised form 9 December 1974)

ABSTRACT

Data were obtained for three High Plains thunderstorms in which penetrations were made of the weak echo region by an instrumented aircraft. The data from one of the cases are presented in detail. Two of the storms were steady state, as revealed by chaff analysis and subsequent subcloud passes. The third storm dissipated during the penetrations. The three storms were each characterized by negatively buoyant air at cloud base. Chaff released into the updrafts of the storms did not decelerate below the level of free convection (LFC). A vertical pressure perturbation gradient, therefore, existed below the LFC and within the weak echo region which acted to accelerate the air parcels in the presence of negative buoyancy. The analysis of the equivalent potential temperature fields for the two steady storm cases revealed considerable entrainment of environment air into the weak echo region. The mixing of the entrained parcels probably caused the observed increase of turbulence with height.

1. Introduction

During the summers of 1968–70, the University of Wyoming operated a research aircraft in conjunction with the Alberta Hail Studies. With the aid of accurate aircraft positioning and high resolution radar, it was demonstrated for the first time that the weak echo region (WER)[2] was indeed an updraft area as Browning and Ludlam (1962) had inferred. However, the characteristics within the WER remained to be determined. The first intentional research flight through a WER was accomplished in Alberta on 28 July 1969 (Marwitz and Berry, 1971). The storm involved was a supercell type (Marwitz, 1972). The aircraft, a B-26 from the Desert Research Institute, contained an onboard radar and was systematically flown through the WER from cloud base (~2.2 km) to 4.9 km MSL.

The onboard radar system was compared with the ground radar to evaluate the relative position-keeping capabilities of the airborne radar. It was demonstrated that the position accuracy of the airborne radar with respect to the echo was ~1 km. This result laid the foundation for the work presented in this paper.

During the summers of 1972 and 1973, the University of Wyoming operated a research equipped Queen Air in participation with the National Hail Research Experiment (NHRE). The Wyoming Queen Air contains a computer controlled digital data system and a real-time display of a complete variety of derived parameters such as potential temperature, equivalent potential temperature, specific humidity, etc. The temperature transducer was a Rosemount system, the dewpoint transducer was a Cambridge system, the turbulence transducer was a MRI Universal turbulence system and the cloud liquid water content (LWC) was measured with a Johnson-Williams system.

The aircraft system was also equipped with a chaff port and an event system. When a packet of chaff was released, the data system was evented so that the precise state parameters of the parcel of air into which the chaff was released are well known. Since the chaff has a slow terminal fall speed (~30 cm/s), the M-33 radar track of the chaff is a 3-D track of a parcel of air within the WER. List *et al.* (1974) have shown that the chaff is not significantly wetted and Marwitz (1973) has shown that the chaff is not significantly iced for ~5 min above the freezing level.

The NHRE field headquarters is located near Grover, Colo. (GRO). One area of participation was the investigation of the dynamics of WER's in High Plains thunderstorms. The WER's of three thunderstorms were successfully penetrated at various altitudes. Two of the storms were steady state, as revealed by chaff trajectories within the WER and subcloud aircraft passes before and after the WER penetrations. The third storm dissipated during the penetrations. Detailed results will be presented and discussed for the case of 24 July 1973. The results from the other case studies will be summarized in Section 4.

---

[1] Present affiliation; INTERA Environmental Consultants, Ltd., Calgary, Alberta.

[2] Since the existence of the "echo-free vault" (Browning and Ludlam, 1962) is a function of the sensitivity of the radar utilized, Chisholm (1973) has chosen to refer to this region as the "weak echo region."

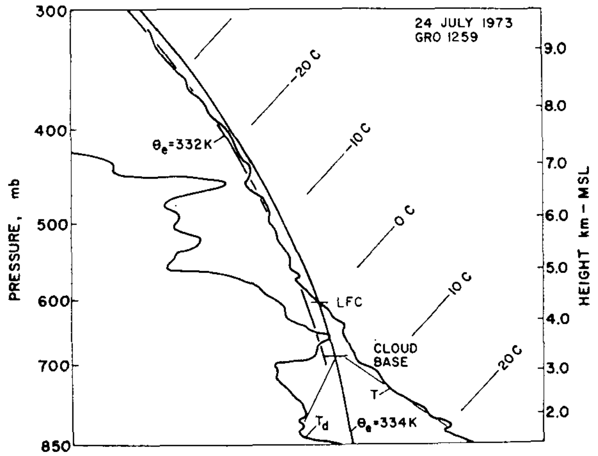

FIG. 1. GRO sounding for 1259 24 July 1973.

2. Environmental conditions—24 July 1973

The environmental conditions surrounding the storm of 24 July 1973 are shown in Fig. 1. This sounding was released[3] at 1259 from GRO and did not indicate the possibility for a great amount of instability. It can be seen from Fig. 3 that the sounding was taken ~60 km ahead of the storm and while it was in existence. A comparison of this sounding and four others taken at GRO before and after 1259 showed consistency among the soundings. In fact, this sounding indicated the most instability of the five.

The low convective temperature (24°C) was realized by 1100 at Sterling, Colo., and resulted in widespread cumulus activity in northeast Colorado.

Figure 2 is the corresponding wind hodograph from the 1259 GRO rawinsonde. Note the light surface winds from the north and generally light winds in the subcloud region. However, the winds above cloud base increased steadily in speed with little veering or backing. The shear value between cloud base and top of the positive energy area (~10.6 km) was 4.3×10^{-3} s^{-1}.

Echo motion of 300° at 9 m/s is noted on Fig. 2. The method used to determine this motion will be discussed in the next section. Note that the echo moved to the right of all environmental winds above cloud base. The winds from chaff packets released at 1326 and 1340 are shown on Fig. 2. Note that the horizontal winds within the WER were similar to the subcloud winds.

3. Aircraft data

The storm formed along the foothills south of Cheyenne and moved toward the southeast. The Wyoming Queen Air arrived in the vicinity of the storm at 1235 and remained until 1340. Figure 3 is the flight track of the Wyoming aircraft from 1235 to 1345. During this time the aircraft made five penetrations of the WER as well as several subcloud updraft passes.

As can be seen from Fig. 3, the motion of the storm was toward the southeast and the orientation of the flight tracks remained the same (E-W). On two separate occasions during the flight, it was noted by the aircraft crew that the controllers at GRO reported the storm moved from 300°. The two comments were made at 1259 and 1338, which bracketed the flight research period.

From the flight track of Fig. 3 it was possible to determine the storm speed. Since the aircraft passes had the same E–W orientation, significant features which repeatedly appeared in the recorded parameters were flagged and plotted with respect to the aircraft track to provide a storm velocity. After plotting several common features with time, a mean velocity of 8.5 m/s was determined. In addition, these signatures moved along lines parallel to 300°, which was the direction given by the GRO controllers.

A time-distance analysis was made on the flight track to determine the aircraft positioning with respect to the storm for the individual passes. The diagram was constructed by noting the time and distance at which the individual passes crossed the line x—x′, which was oriented along 300°. Passes A–E were selected for intensive discussion since they were near the line and could be vertically collocated in order to analyze the WER with respect to the storm motion.

The time-distance analysis could also be used to determine the storm speed. This was 9 m/s, which agrees very well with the speed of 8.5 m/s found from Fig. 3. While the storm motion was not directly determined from radar data, it was felt that the motion, as determined, was satisfactory for this study.

The cloud base as observed by the aircraft is included in Fig. 1 along with the environmental sounding and line of θ_e=332 K and 334 K. The state parameters in the updrafts at cloud base were θ=310 K and q=8 g kg^{-1}. Note that the updrafts at cloud base were 1–2°C colder than the environment.

This particular storm was the last storm on the southwest end of a line of storms oriented along a

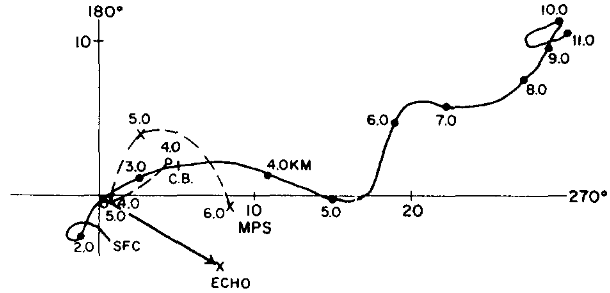

FIG. 2. Wind hodograph of the GRO 1259 sounding. Echo motion is indicated by an X. x--x is the chaff winds for 1326, and ● — ● the chaff winds for 1340.

[3] All times are Mountain Standard Time.

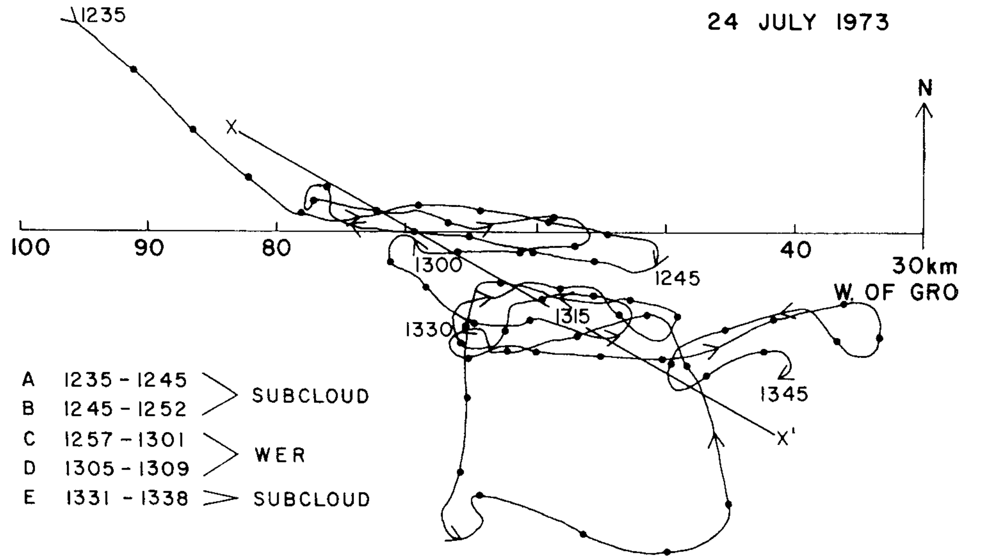

FIG. 3. Aircraft track from 1235–1345. The list to the left of the figure indicates the passes used in the analysis. The line x−x′ was along 300° and was used in a time-distance analysis to determine storm speed.

NE–SW line. A photograph taken at 1252 as the aircraft first approached the storm confirmed that this storm was isolated except on the northeast side where it was attached to the line. Near the end of the series of passes another storm developed at the southwestern end of the line.

Figure 4 (a–c) depicts the analog traces of equivalent potential temperature (θ_e), potential temperature (θ), specific humidity (q), indicated turbulence (IT), and updrafts (W) for passes B, D, and E respectively. IT equals $\epsilon^{\frac{1}{3}}\rho/\rho_0$, where ρ is density at flight altitude, ρ_0 is density at sea level and ϵ is the eddy dissipation rate. The updrafts were obtained using the aircraft as the sensor and for those flight periods when the heading and airspeed were approximately constant (Marwitz, 1972). The time has been appropriately inverted so that the left side of the figures is the southwest side of the storm. Aircraft passes through or underneath the edge of the storm are noted.

Figure 4, a, depicts the traces for pass B (1245–1252). Note the lack of turbulence (IT) and the high θ_e values in the updrafts and the sharp boundary in the state parameters between the updrafts and the downdrafts. The updrafts are charcterized by low θ (310 K) and high q (7.5 g kg^{-1}). The source of this updraft air was near the surface. Higher values of IT (>3 cm$^{\frac{2}{3}}$/s) were observed between the individual cells.

Figure 4, b, is the second WER penetration (pass D) and was made from 1305 to 1309. The penetration was made at ~4.3 km, which, as seen in Fig. 1, was near the LFC and 1.0 km above cloud base. During pass C (below the LFC), θ was out of phase with θ_e, while θ was in phase with θ_e during this pass. The LWC and θ_e within the main updraft core were less than adiabatic and the parameters fluctuated considerably, indicating entrainment.

After pass D, the aircraft descended to cloud base to continue the inflow study. Fig. 4, c, depicts the subcloud conditions for pass E (1331–1338). Although a new storm had developed on the SW end of the line, the storm that was penetrated was still active and essentially unchanged.

Figure 5 depicts the θ_e traces from passes A–E. The lower three traces were made near cloud base (~3.4 km) and the two WER penetration passes are stacked above the cloud base traces. The altitudes of entry and exit of the WER are noted. $\theta_e > 332$ K is shaded. Note the decrease of θ_e with height, both for $\theta_{e\,\max}$ and $\bar{\theta}_e$. Table 1 contains several characteristics of each pass and also reflects this decrease of θ_e with height. The traces of θ_e, θ, q, and LWC for pass C were relatively smooth, while the traces for pass D fluctuated considerably.

Figure 6 depicts the IT traces for passes A–E. Note the smooth air in the updrafts and the turbulent transition between the environment and the updraft air. The turbulence in the updraft was seen to increase with height.

TABLE 1. Table of height, $\theta_{e\,\max}$, $\bar{\theta}_e$, IT$_{\max}$ and $W_{\max}$ for passes A–E.

Pass	Height km	$\theta_{e\,\max}$ K	$\bar{\theta}_e$ K	IT$_{\max}$ cm$^{\frac{2}{3}}$ s^{-1}	$W_{\max}$ m s^{-1}
A	3.3	334.1	332.5	2.5	7.0
B	3.3	333.7	332.5	2.0	5.0
C	3.6	332.3	330.0	3.0	3.0
D	4.3	332.1	330.0	4.0	6.5
E	3.3	333.4	332.0	2.0	—

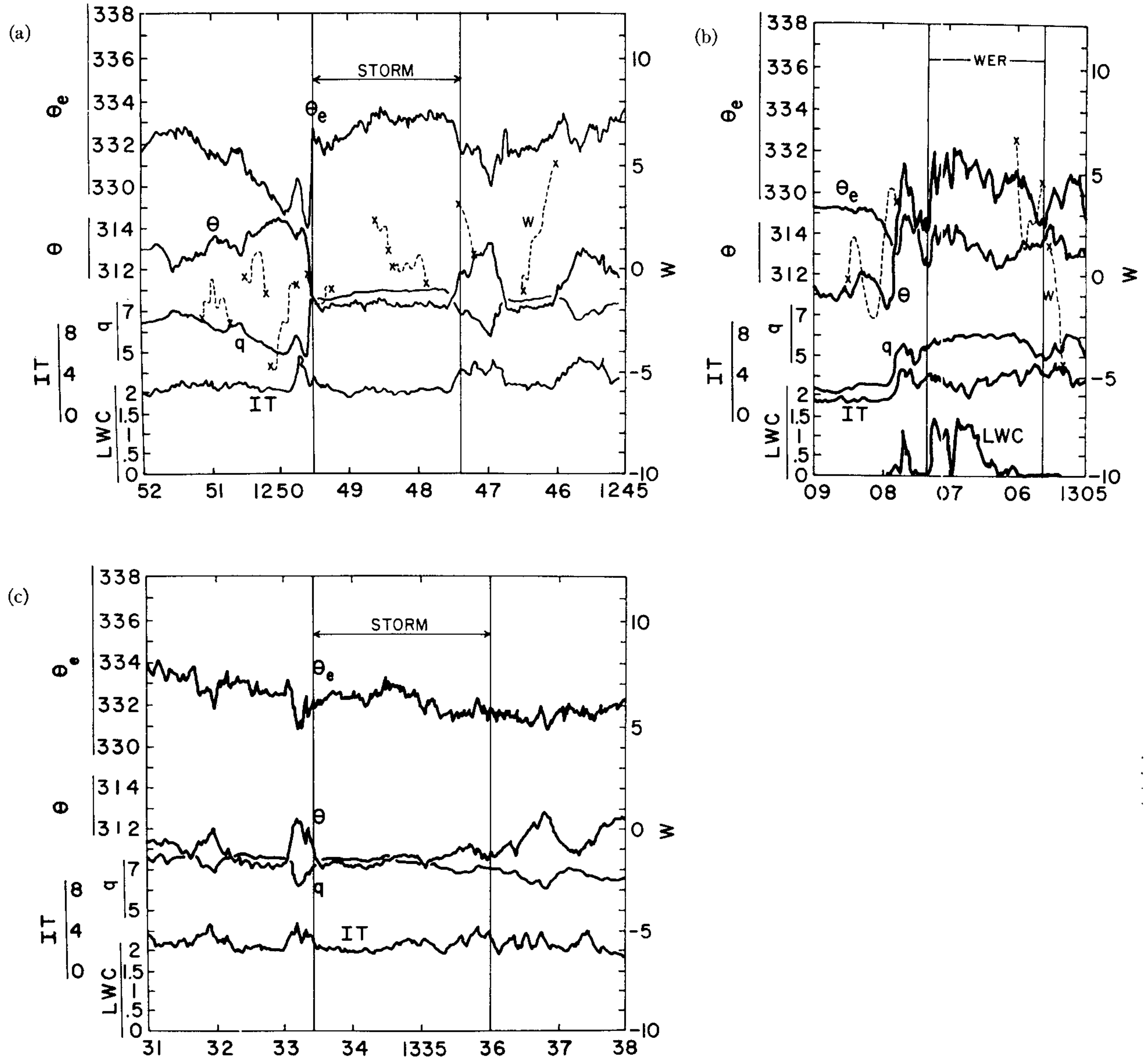

FIG. 4. Traces of equivalent potential temperature (θ_e, K), potential temperature (θ, K), specific humidity (q, g/kg), indicated turbulence (IT, $cm^{2/3}/s$), vertical motion (W, m/s) and liquid water content (LWC, g/m^3) for (a) pass B (1245–1252) taken near cloud base (3.4 km): (b) pass D (1305–1309) taken between 4.2 and 4.5 km: (c) pass E (1430–1438) taken at cloud base (3.4 km).

From Figs. 5 and 6 there appeared to be substantial entrainment into the WER and a corresponding breakdown of the smooth flow field with height as indicated by the decrease in θ_e, the increase in horizontal variability in θ_e and LWC, and the increase in turbulence.

An attempt was made to construct a vertical section through the updraft core of WER (see Fig. 7). The profile is along the direction of motion of the storm. Passes A–E were collocated vertically, approximately 2 km from the precipitation wall based on the chaff data and time-distance analysis. The three subcloud passes showed a maximum θ_e of 334 K, which, referring to the vertical sounding of θ_e, originated near the surface. Passes C and D had a maximum θ_e of 332 K. The three other WER penetration passes were positioned with respect to the echo using the time-distance analysis. The trajectories of the chaff packets released at cloud base subsequent to the WER penetrations were added to Fig. 7 to provide information on the updraft slope. The trajectories are with respect to the moving storm. The analysis of the θ_e field was made consistent with the chaff trajectories. Of particular interest was the pattern of decreasing θ_e with height. In fact, the surface value of 334° barely extended 500 m above cloud base. It is apparent that substantial entrainment was occurring in this cell.

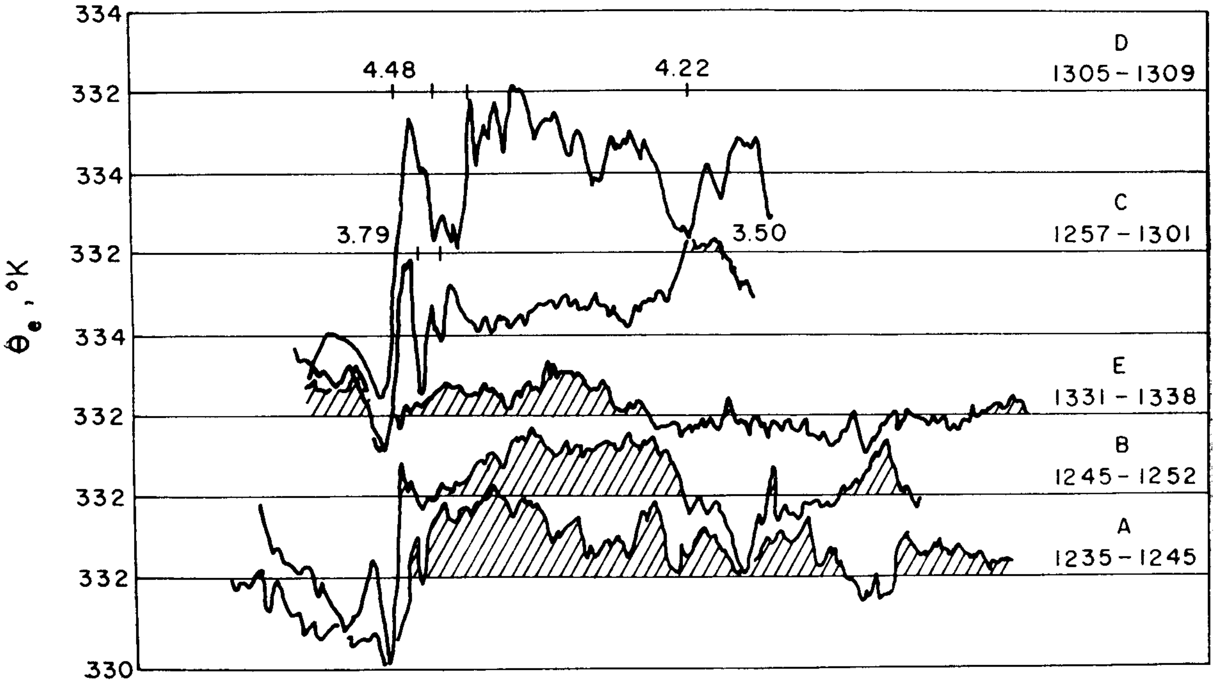

FIG. 5. Collocated traces of θ_e from passes A–E. Shaded regions correspond to $\theta_e > 332$ K. The WER entry and exit altitudes and locations are noted.

Figure 8 shows the updraft profiles for the two packets of chaff released in this storm. Both packets of chaff were released subsequent to the WER penetrations. The vertical velocity profile for the packet released at 1326 is similar to the profiles described by Marwitz (1973). Note the region of acceleration below 6.0 km, then the deceleration prior to echo entry.

4. Summary

Aircraft and chaff data were presented for the WER penetration study of 24 July 1973. Similar indications of entrainment into the WER were found for the case of 30 June 1973 (Grandia, 1973). The storm on 30 June produced 2 cm diameter hailstones, but the storm on

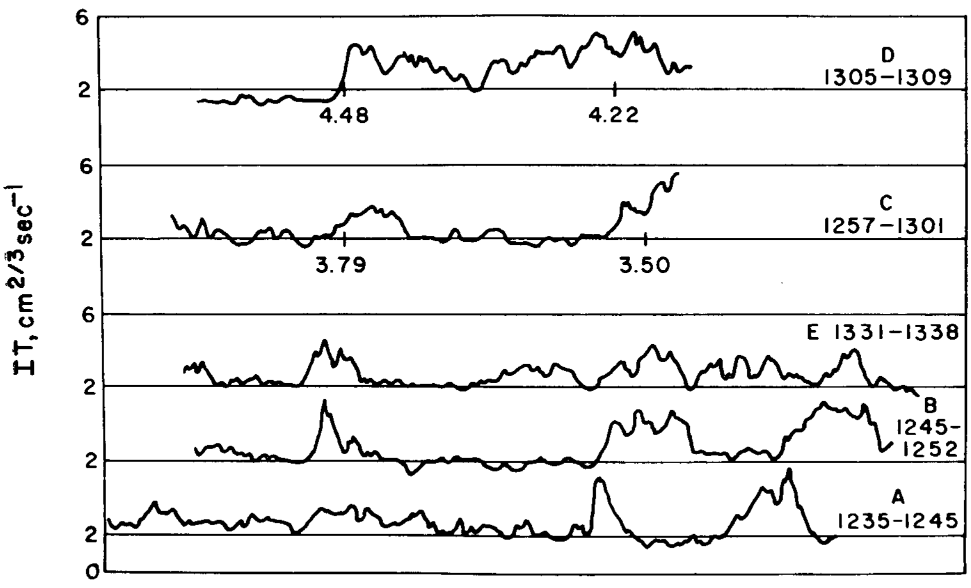

FIG. 6. Collocated traces of IT from passes A–E.

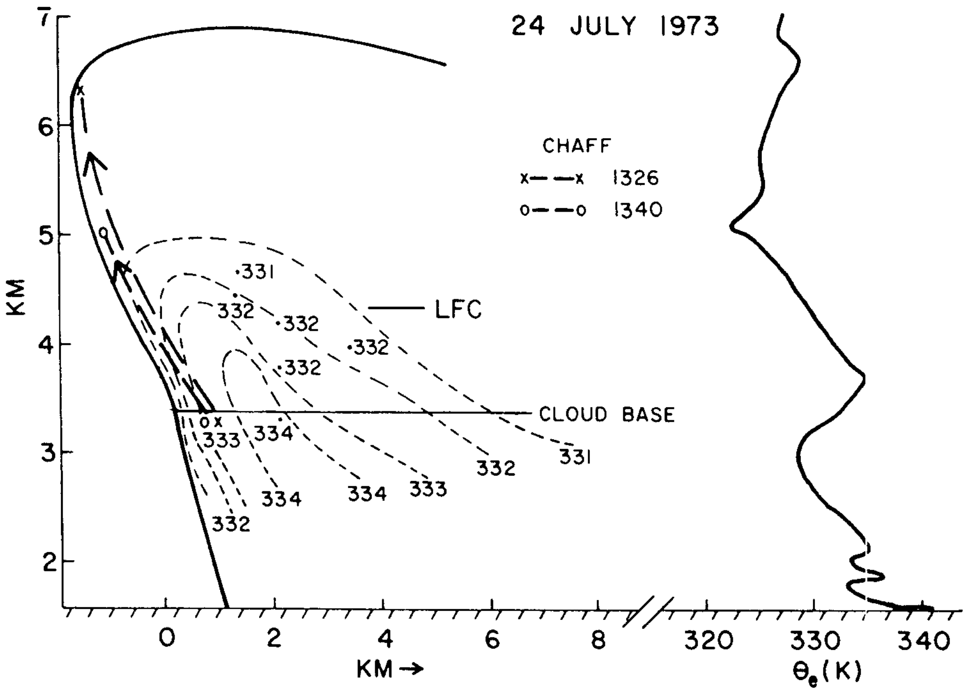

FIG. 7. Synthesis of aircraft, chaff and sounding data. x—x is trajectory of chaff released at 1326. o—o is trajectory of chaff released at 1340. Vertical θ_e profile is from the GRO 1259 rawinsonde.

24 July was not thought to have produced any hail at the ground. A third penetration study, 19 July 1972, was consistent with the other two cases, but since the storm dissipated during the last penetrations the results were ambiguous.

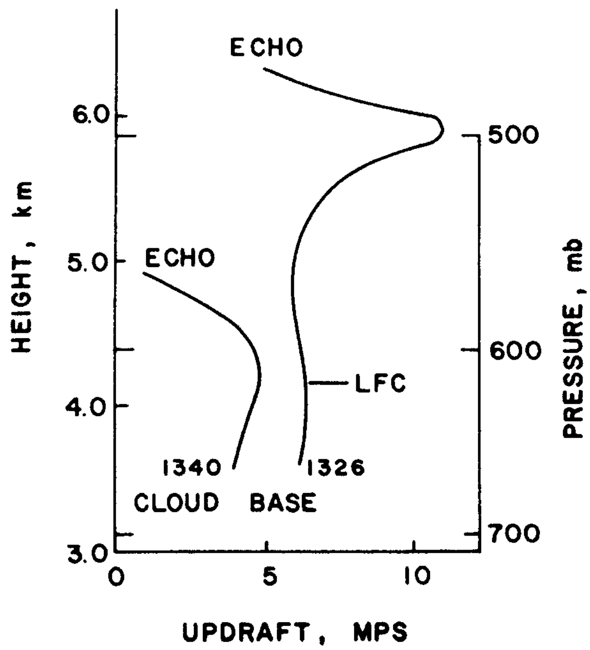

FIG. 8. Updraft profiles for the chaff packets released at 1326 and 1340 on 24 July 1973.

Each of the three storms were characterized by updrafts at cloud base which were 1–3°C colder than the environment. Such a characteristic cloud base updraft has been observed in many High Plains thunderstorms. Of the eight storms studied by Marwitz (1973), all but one had cold updrafts at cloud base. Davies-Jones and Henderson (1973) found this same characteristic from radiosondes released into Oklahoma thunderstorms.

The vertical velocities measured by the chaff did not decrease in the negatively buoyant updrafts near cloud base for any of the storms in the present study. In fact, at least one chaff track for each storm measured an increase of vertical velocity with height. It is also significant to note that at least one chaff track for each storm indicated a substantial decrease in updrafts just prior to entering the echo near the middle part of the cloud. These results are in agreement with Sulakvelidze *et al.* (1967) and Marwitz (1973).

An analysis of θ_e at the various heights within the WER indicated that a substantial amount of entrainment occurred in the WER. The fluctuating nature of the horizontal profiles of θ_e and LWC suggested that large eddies (1–2 km) were entrained and had begun to mix with the updraft air.

All but one of the passes through the WER were made below the LFC. The turbulence data indicated that the turbulence increased with height between the cloud base and the LFC. It would seem that the increased turbulence was caused by the interaction between the updraft and entrained air. The one pass above the LFC revealed a decrease in turbulence. Its significance is not known.

5. Conclusions

The observations contained in Section 4 are synthesized in a physical model of the WER. Figure 9 contains schematic vertical profiles of various parameters associated with thunderstorms on the High Plains. The sounding is typical of the environmental conditions surrounding High Plains thunderstorms. The observed temperature, moisture and pressure in the updrafts at cloud base reveal that the updrafts are 1–3°C colder than the environment and the updrafts originate near the ground. The vertical profile of the thermal buoyancy force (gT'/T_e) as determined from virtual temperatures for an unentrained parcel is as shown. Note the negative thermal buoyancy from the surface to the LFC and the large positive region above the LFC. If thermal buoyancy were the primary vertical force, the updrafts (W) would decelerate with height below the LFC and increase rapidly with height above the LFC. Also, the maximum updrafts would typically occur near the tropopause. Note, however, that the updrafts accelerate below the LFC and decelerate just prior to entering the echo near the middle of the cloud. The perturbation analysis of the equation of motion as presented by List and Lozowski (1970) can explain the observed updraft profile of Fig. 9. The vertical equation of motion is

$$\frac{dw}{dt} = -\frac{1}{\rho_e}\frac{\partial P'}{\partial z} - \left(\frac{P'}{P_e} - \frac{T'}{T_e}\right)g + d + f_z \quad (1)$$

and the horizontal equation of motion is

$$\frac{du}{dt} = -\frac{1}{\rho_e}\frac{\partial P'}{\partial x} + f_x, \quad (2)$$

where Q' denotes the perturbation quantity, Q_e denotes the environmental quantity, d is hydrometeor drag and f is frictional drag. The first term in Eqs. (1) and (2) is the acceleration due to the gradient of pressure perturbation and the second term in Eq. (1) is the pressure [$g(P'/P_e)$] and temperature [$g(T'/T_e)$] components of buoyancy.

Assuming no drag and no friction, a pressure perturbation of 1 mb will cause the horizontal velocity of an air parcel to change by ~14 m/s while a 4 mb perturbation will cause a change of 28 m/s. The horizontal velocities observed by the chaff indicates that changes of 5 to 10 m/s are common with 15 m/s being an extreme value. Pressure perturbation deficits at cloud base are, therefore, inferred from the chaff and state parameters to be on the order of 1 mb. Typical pressure perturbations in mesolows at the surface are typically observed to be ~0.5 mb and mesohighs are typically ~4 mb (Fujita, 1963).

Typical storms in northeastern Colorado have a virtual temperature at cloud base which is ~2°C colder

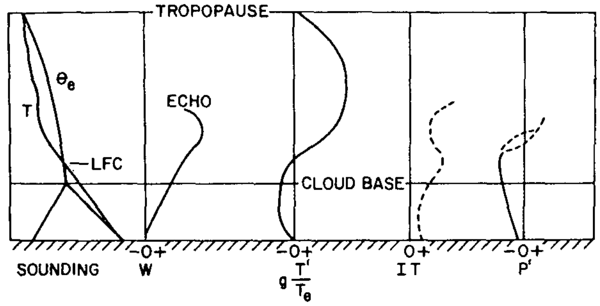

FIG. 9. Conceptual model of turbulence (IT) and pressure perturbation (P') as revealed by the vertical velocity (W) and thermal buoyancy [$g(T'/T_e)$] for a typical High Plains thunderstorm sounding.

than the environment (~285 K). The pressure at cloud base is ~1 mb less than the environment (650 mb). The thermal buoyancy is −0.007 g while the pressure buoyancy is +0.002 g. The updrafts are, therefore, negatively buoyant. Since the chaff is almost always observed to accelerate in the vertical, the vertical gradient of pressure perturbation (the first term in Eq. 1) must overcompensate for the negative buoyancy. An additional decrease of 1 to 1.5 mb between the cloud base and LFC is consistent with the available observations.

The depicted vertical pressure perturbation deficit is typically observed at the surface as a mesolow. The deficit increases with height below the LFC such that the updrafts are still negatively buoyant but with such a vertical gradient that the chaff is accelerated as observed. The deceleration of the chaff just prior to entering the echo may be caused by a rapid reversal of the pressure perturbation gradient and/or entrainment. Both seem likely from the data.

The vertical profile of turbulence is indicated in Fig. 9.

The results presented indicate considerable entrainment into the WER. It seems likely that the pressure deficit induces horizontal entrainment of large eddies of dry air into the updraft and the WER. The entrainment is seen by the decrease of θ_e with height in the WER.

An immediate consequence to the above model is that a WER not characterized by cold updrafts at cloud base and, hence, by a pressure deficit, would entrain less outside air. While penetrations have not been made within the WER of such storms, Marwitz (1973) has shown that for the one case of chaff profiles within such a storm, the chaff did not decelerate prior to echo entry, i.e., the chaff continued to accelerate from the time of chaff release until the radar lost track. Thus, chaff tracks have only been obtained in one storm which did not require a pressure perturbation term to explain the vertical velocity profile.

Acknowledgments. Special thanks go to the team of engineers, technicians, programmers, draftsman, and typists in the Department of Atmospheric Science at the University of Wyoming. Without their enthusiastic support, this research would not be possible.

This research was performed as part of the National Hail Research Experiment, managed by the National Center for Atmospheric Research and sponsored by the Weather Modification Program, Research Applications Directorate, National Science Foundation.

REFERENCES

Browning, K. A., and F. H. Ludlam, 1962: Airflow in convective storms. *Quart. J. Roy. Meteor. Soc.*, **88**, 117–135.

Chisholm, A. J., 1973: Alberta hailstorms. Part I: Radar case studies and airflow models. *Meteor. Monographs*, **14**(36), 1–36.

Davies-Jones, R. P., and J. H. Henderson, 1973: Characteristics of thunderstorm updraft soundings. Preprints, Eighth Conf. on Severe Local Storms, Boston. Amer. Meteor. Soc., 1–15.

Fujita, T., 1963: Analytical mesometeorology: A review. *Meteor. Monographs*, **5**(27), 77–128.

Grandia, K. L., 1973: Aircraft observations within the weak echo region of High Plains thunderstorms. M.Sc. thesis, Department of Atmospheric Science, University of Wyoming, 90 pp.

List, R., T. B. Low, and J. D. McTaggart-Cowan, 1974: Collisions of raindrops with chaff. *J. Appl. Meteor.*, **13**, 796–799.

——, and E. P. Lozowski, 1970: Pressure perturbations and buoyancy in convective clouds. *J. Atmos. Sci.*, **27**, 168–170.

Marwitz, J. D., 1972: The structure and motion of severe hailstorms, Parts I, II, III. *J. Appl. Meteor.*, **11**, 166–201.

——, 1973: Trajectories within the weak echo regions of hailstorms. *J. Appl. Meteor.*, **12**, 1174–1182.

——, and E. X. Berry, 1971: The airflow within the weak echo region of an Alberta hailstorm. *J. Appl. Meteor.*, **10**, 487–492.

Sulakvelidze, G. K., H. Sh. Biblashvili, and V. F. Lapcheva, 1967: *Formation of Precipitation and Modification of Hail Processes.* Translated by Israel Program for Scientific Translations, Jerusalem, 208 pp.